Published in final edited form as:
Dev Biol. 2008 December 15; 324(2): 245–257. doi:10.1016/j.ydbio.2008.09.014.

The MIG-15 NIK kinase acts cell-autonomously in neuroblast polarization and migration in *C. elegans*

Jamie O. Chapman, **Hua Li**[1], and **Erik A. Lundquist**[2]
Department of Molecular Biosciences, University of Kansas, 1200 Sunnyside Ave., Lawrence, KS 66045-7534

Abstract

Cell migration is a fundamental process in animal development, including development of the nervous system. In *C. elegans*, the bilateral QR and QL neuroblasts undergo initial anterior and posterior polarizations and migrations before they divide to produce neurons. A subsequent Wnt signal from the posterior instructs QL descendants to continue their posterior migration. Nck-interacting kinases (NIK kinases) have been implicated in cell and nuclear migration as well as lamellipodia formation. Studies here show that the *C. elegans* MIG-15 NIK kinase controls multiple aspects of initial Q cell polarization, including the ability of the cells to polarize, to maintain polarity, and to migrate. These data suggest that MIG-15 acts independently of the Wnt signal that controls QL descendant posterior migration. Furthermore, MIG-15 affects the later migrations of neurons generated from Q cell division. Finally, a mosaic analysis indicates that MIG-15 acts cell autonomously in Q descendant migration.

Introduction

Cell migration is a key morphogenetic process in animal development. Migration of neurons and their precursors are important in forming distinct cortical layers and functional nuclei of neurons in the developing vertebrate central nervous system. In *C. elegans*, the bilateral Q neuroblasts, born in the posterior-lateral region of the animal, and their neuronal descendants execute long-range anterior and posterior migrations in the first larval stage (Chalfie and Sulston, 1981; Sulston and Horvitz, 1977). After hatching, QL and QR undergo initial, short-distance posterior and anterior migrations, respectively, after which they divide. QL and descendants encounter a Wnt signal in the posterior which, via canonical Wnt signaling, drives expression of the *mab-5 Hox* gene in QL descendants (Chalfie et al., 1983; Eisenmann and Kim, 2000; Harris et al., 1996; Herman, 2001; Kenyon, 1986; Korswagen et al., 2000; Salser and Kenyon, 1992; Whangbo and Kenyon, 1999). *mab-5* expression in QL descendants causes them to continue posterior migration. QL generates three neurons: SDQL and PVM reside near the site of Q cell birth in the left postdeirid ganglion, and PQR migrates posteriorly into the phasmid ganglion in the tail (Sulston and Horvitz, 1977; White et al., 1986). In mutants affecting Wnt signaling and in *mab-5* mutants, QL descendants reverse their direction of migration and migrate anteriorly instead of posteriorly (Chalfie et al., 1983; Eisenmann, 2005; Kenyon, 1986; Salser and Kenyon, 1992). QR, which migrates a short distance anteriorly

[2]Author for correspondence (email: erikl@ku.edu).
[1]Current Address, Department of Cell Biology, Yale University, New Haven, CT 06510

and divides, does not respond to the posterior Wnt signal and does not express *mab-5*. Consequently, the three neurons generated by QR (SDQR, AVM, and AQR) migrate anteriorly. AQR migrates the longest distance into the head of the animal in the anterior deirid ganglion.

Mutations in *unc-40*, which encodes the netrin receptor (Keino-Masu, 1996), and *dpy-19*, which encodes a novel, conserved transmembrane protein (Honigberg and Kenyon, 2000), randomize initial Q cell polarization, and mutations in *unc-73*, which encodes the RacGEF Trio (Steven et al., 1998), affect the ability of Q cells to polarize and migrate (Honigberg and Kenyon, 2000). The transmembrane molecule MIG-13 might be involved in establishing an anterior-posterior guidance system that is required for anterior migration of QR descendants (Sym et al., 1999). These studies have identified potential guidance ligands, guidance receptors, and cellular effectors that mediate Q cell migration. While much has been learned about Q cell migration, many of the mechanisms that control Q cell polarity and Q cell migration remain to be elucidated.

Previous studies have implicated the Nck-interacting kinases, NIK kinases, as regulators of a variety of morphogenetic events involving cytoskeletal regulation and cell shape. In Drosophila, the NIK molecule Misshapen is involved in cell and nuclear migration, interacts with a JNK/MAPK kinase pathway, and controls axon pathfinding (Houalla et al., 2005; Su et al., 2000; Su et al., 1998). Vertebrate studies have also implicated NIK kinases in cell migration and as acting with JNK signaling and integrins (Becker et al., 2000; Xue et al., 2001). In cultured cells, treatment with EGF and PDGF leads NIK kinase-dependent phosphorylation of ERM proteins responsible for actin organization and lamellipodium formation (Baumgartner et al., 2006).

mig-15 encodes a *C. elegans* Nck-interacting kinase (NIK) (Poinat et al., 2002; Su et al., 1997). MIG-15 contains an N-terminal pak/ste20-type serine/threonine kinase domain followed by a proline-rich region. The C-terminus of MIG-15 contains a citron-NIK homology domain (CNH), a conserved domain thought to interact with Rac GTPases and β1 integrin (Figure 1). Mutations in *mig-15* cause defects in axon pathfinding as well as Q descendant migration (Poinat et al., 2002; Shakir et al., 2006). *mig-15* acts upstream of *mab-5*, as the constitutively-active *mab-5(e1751)* allele, which causes constitutive *mab-5* expression in both QL and QR descendants, rescues the anterior QL descendant migration defects in *mig-15* mutants (i.e. in *mig-15; mab-5(e1751)* doubles, QL descendants always migrate to the posterior) (Shakir et al., 2006).

Previous work showed that MIG-15 was required for initial Q cell migration (Williams, 2002), but it is not clear if *mig-15* also affects Q cell polarization or if *mig-15* might also affect later Wnt-related events. Furthermore, it is not clear if MIG-15 acts in the Q cells and descendants or in another tissue such as a substrate for Q descendant migration. Described here are studies showing that MIG-15 controls initial Q cell polarization and maintenance of polarity in addition to affecting Q cell and Q descendant migration. Furthermore, analysis of *mig-15* genetic mosaics was consistent with a cell-autonomous role of MIG-15 in AQR and PQR migration.

Results

The MIG-15 NIK kinase

Previous studies showed that mutations in the *mig-15* gene, which encodes a molecule similar to vertebrate Nck-interacting kinase (NIK) (Poinat et al., 2002) (Figure 1), perturbed the migrations of Q cell descendants (Shakir et al., 2006). As shown in Figure 1, the *qid-7 (mu327)* and *qid-8(mu342)* mutations previously found to perturb Q descendant migration (Ch'ng et al., 2003) were new alleles of *mig-15* (see Materials and Methods). The hypomorphic

rh148 mutation is a missense mutation in the ATP-binding-pocket of the kinase domain, and the stronger allele *rh80* is a premature stop codon after the kinase domain (Figure 1) (Shakir et al., 2006). While *rh80* causes a premature stop, it might have residual *mig-15* activity and might not represent a null. However, *rh80* causes a more severe phenotype than *rh148* and represents a strong loss-of-function of the *mig-15* gene.

Imaging initial QL and QR migrations

Initial Q cell migrations were visualized in wild-type and *mig-15* mutants. In the wild-type L1 larva, QL and QR undergo initial posterior and anterior migrations, respectively, followed by cell division (Sulston and Horvitz, 1977). QL descendants then receive a Wnt signal from posterior cells that directs further posterior migrations of the QL descendants by activating the *mab-5 Hox* gene (Maloof et al., 1999; Salser and Kenyon, 1992; Whangbo and Kenyon, 1999). QR descendants do not respond to this Wnt signal, do not express *mab-5*, and migrate anteriorly (Salser and Kenyon, 1992).

The initial, Wnt-independent migrations of the Q neuroblasts were imaged using an *scm promoter::gfp::caax* transgene. L1 larvae were synchronized by hatching (see Materials and methods), and Q neuroblasts were observed at different timepoints after hatching. Results presented here were consistent with other observations of initial Q cell migration (Honigberg and Kenyon, 2000).

At hatching, the Q cells were unpolarized and were located between the V4 and V5 seam cells (Figures 2A and B). At 1–2.5h after hatching, QL sent a process posteriorly over the left V5 seam cell (V5L) and QR sent a process anteriorly over the right V4 seam cell (V4R) (Figures 2C and D). In most cases, the processes extended greater than half the distance over the respective V cells. The Q cell processes resembled the leading edges of migrating cells in other systems and displayed lamellipodia-like protrusions with filopodia-like extensions (Figures 2C and D). These anterior and posterior protrusions persisted, and at 3–3.5h, the cell bodies of QL and QR followed the protrusions and migrated over their respective seam cells such that QL was located over V5L and QR was located over V4R (Figures 2E and F). At 4–4.5h after hatching, QL and QR underwent mitosis, producing anterior and posterior daughters (QL.a/QL.p and QR.a/QR.p) located above V5L and V4R, respectively (Figures 2G and H). A schematic diagram of wild-type initial Q cell migration is shown in Figure 2I. To summarize, the Q cells underwent an initial polarization (QL posteriorly and QR anteriorly); the cell bodies of QL and QR migrated posteriorly and anteriorly over V5L and V4R, following the initial protrusions; and QL and QR underwent mitosis above V5L and V4R.

MIG-15 is required for Q cell polarization and maintenance of Q cell polarity

mig-15(rh80) causes a premature stop codon and is a strong loss-of-function allele, and *mig-15 (rh148)* is a missense mutation affecting the ATP-binding pocket of the kinase domain (Figure 1) (Shakir et al., 2006). Shown here and in Shakir et al., 2006, Q descendant migration defects of *mig-15(rh148)* are generally less severe than *mig-15(rh80)*. The Unc Pvl Dpy phenotype of *mig-15(rh148)* was also less severe than *mig-15(rh80)* (data not shown), suggesting that *mig-15 (rh148)* might cause weaker loss of *mig-15* function than *mig-15(rh80)*.

Q cell polarization was assayed in *mig-15(rh148)* and *mig-15(rh80)*. At hatching, Q cell position and morphology in both mutants resembled wild-type (n = 35 for each) (data not shown). Initial QL and QR polarization in the hypomorphic *mig-15(rh148)* mutant occurred apparently normally at 1.5–2.5h after hatching (Figures 3A and B). The posterior and anterior protrusions extended distances over V5L and V4R similar to wild-type. Often, *mig-15 (rh148)* protrusions displayed more filopodia-like extensions than did wild-type (Figures 3A and B).

In *mig-15(rh80)* mutants, the time required for polarization and division was increased compared to the *scm::gfp::caax* strain alone. This was likely due to a general developmental delay in *mig-15(rh80)*, as the time to complete larval development was increased in these mutants (data not shown). At 2–2.5h after hatching, the equivalent of 1–2.5h in wild-type, the QL and QR cells always appeared to polarize in the correct direction. However, the polarizations were abnormal in that the protrusions did not extend as far toward the posterior or anterior over the V5L and V4R seam cells, usually less than half the length of the V cells (compare Figures 4A and B with Figures 2C and D). All *mig-15(rh80)* animals displayed reduced protrusion, and QL and QR were equally affected. While *mig-15(rh80)* Q cells failed to fully polarize, the direction of initial Q cell polarization was not affected.

When observed later at 3–3.5h after hatching, at a time when wild-type Q cells began their migrations over the V cells, some *mig-15* mutant Q cells had failed to remain properly polarized (Figure 3 and Table 1). Some cells remained polarized in the correct direction but sent branches in the other direction (Figure 3C–D and 4C), some were polarized to both the anterior and posterior (Figure 3E), and some were not polarized strongly in either the anterior or posterior direction (Figure 3F–H and 4D).

MIG-15 is required for Q cell migration

In wild-type, the QL and QR cell bodies follow the posterior and anterior protrusions and migrate over V5L and V4R. In *mig-15* mutants, Q cells often failed to fully migrate over the respective seam cells before division (4–4.5h after hatching). Some Q cells did not migrate at all and divided between V4 and V5 (Figure 3I and Figure 4E and F). Some Q cells had migrated partially and divided on the edges of the V cells (Figure 3J). The percentages of Q cells that failed to migrate properly are shown in Figure 3K and Figure 4G. While the proportions of QL and QR that failed to migrate properly in *mig-15(rh148)* were similar, QRs always migrated some distance over V4R as shown in Figure 3J whereas QLs often failed to migrate any distance before division as shown in Figure 3I. QL and QR were equally affected in *mig-15(rh80)*.

Interestingly, some QL cells (5%) in *mig-15(rh148)* were observed that, instead of having migrated posteriorly over V5L, migrated anteriorly and divided over V4L (Figure 3K), suggesting that a failure to maintain polarity could result in a repolarization and migration in the opposite direction. This is consistent with the earlier observation that some QL cells were apparently polarized in both the anterior and posterior directions (Figure 3E). Anterior QL division was not observed in *mig-15(rh80)*, possibly because of the more severe general defects in polarization and migration in this mutant. MIG-15 was previously shown to affect Q migration (Williams, 2002). Data reported here indicate that *mig-15* is required for the ability of Q cells to polarize and to maintain polarity, in addition to being required for Q cell migration. Initial direction of Q cell polarization was not affected by *mig-15(rh148)*or *mig-15(rh80)*. While *mig-15(rh80)* causes a premature stop, it might not represent a complete loss of function. Therefore, it is possible that complete loss of *mig-15* function might also affect direction of Q cell polarization.

Canonical Wnt signaling does not affect initial Q cell migration

Mutations in canonical Wnt signaling cause reversal of QL descendant migration (Eisenmann, 2005). Canonical Wnt signaling is thought to act after QL cell polarization and migration. To confirm that canonical Wnt signaling did not affect early Q cell polarization and migration, these cells were analyzed in canonical Wnt signaling mutants. The initial polarizations and migrations of QL and QR in *lin-17(e1456)/Frizzled* (Sawa et al., 1996) and *bar-1(ga80)/β-catenin* (Eisenmann et al., 1998) were similar to wild-type (data not shown). Furthermore, QL and QR divided atop V5L and V4R in these mutants, indicating that initial QL and QR migrations were not affected by *lin-17(e1456)* and *bar-1(ga80)* (Figure 5). *bar-1(ga80)* is

thought to be a strong loss-of-function allele, and *bar-1* encodes the only β-catenin involved in canonical Wnt signaling in *mab-5* activation (Herman, 2003; Korswagen et al., 2000; Maloof et al., 1999; Natarajan et al., 2001). These data confirm that complete loss of canonical Wnt signaling does not affect initial Q cell polarization and migration and that *mig-15* acts in a canonical Wnt-independent manner in Q cell polarization and migration.

mab-5 expression in QL is reduced in *mig-15* mutants

A full-length *mab-5* coding region fused to *gfp (mab-5::gfp)*, shown previously to report MAB-5 expression (Cowing and Kenyon, 1996; Forrester et al., 2004), was used to visualize MAB-5 protein expression in wild-type and *mig-15(rh148)*. In wild-type, MAB-5::GFP expression was observed in QL descendants in 37/51 animals (67%), whereas 33/75 *mig-15 (rh148)* animals (44%) showed visible MAB-5::GFP in the QL descendants ($p = 0.01$). This approximately 35% reduction in MAB-5 expression in *mig-15(rh148)* is in line with the previously-reported percentage of PQR direction of migration defects. Furthermore, *qid-7 (mu327)* and *qid-8(mu342)*, alleles of *mig-15* as described above, caused reduced MAB-5::GFP expression in QL descendants (Ch'ng et al., 2003).

The Q descendants AQR and PQR reverse direction of migration in *mig-15* mutants in a *mab-5*-dependent manner

The migrations of Q cell descendants AQR (QR.ap) and PQR (QL.ap) were analyzed in *mig-15* mutants. Previous studies utilized an *osm-6::gfp* transgene, expressed in all ciliated sensory neurons including AQR and PQR, to score AQR and PQR position (Shakir et al., 2006). In work described here, a transgene consisting of the *gcy-32* promoter driving *gfp* expression (*gcy-32::gfp)* was used to score AQR and PQR. *gcy-32::gfp* was expressed in AQR and PQR after completion of their anterior and posterior migrations (Figure 6A and D) (Yu et al., 1997). *gcy-32::gfp* was also expressed in the non-Q cell-derived URX neurons in the head, one on the left and one on the right (Figure 6A). The posterior migration of PQR was dependent upon Wnt signaling, as mutations in the canonical Wnt pathway (*egl-20(mu39)/Wnt*, *lin-17 (e1456)/Frizzled*, and *bar-1(ga80)/β-catenin*) caused PQR to migrate anteriorly instead of posteriorly and had no effect on AQR migration (Figure 7). Previous studies indicated that in *egl-20* mutants, the QR descendants AVM and SDQR stopped short of their normal anterior positions (Harris et al., 1996; Zinovyeva et al., 2008). We saw no effect on AQR position in *egl-20(mu39)*. Wnt activity in the control of AVM/SDQR placement is complex, as multiple Wnts are required for AVM/SDQR migration and they can have opposing activities, as *lin-44* partially suppresses AVM/SDQR defects of *egl-20* (Zinovyeva et al., 2008). AQR migrates further to the anterior than AVM/SDQR, and possibly AQR migration does not rely on these Wnt interactions in the same manner as AVM/SDQR for its final position.

In both *mig-15(rh148)* and *mig-15(rh80)*, PQR reversed direction of migration to migrate anteriorly (39% and 47%, respectively) (Figure 6E and F). A small but significant proportion of AQR neurons migrated posteriorly into the phasmid ganglion in *mig-15(rh80)* (6%) (Figure 6F and Figures 8A and B), a defect never observed in wild-type or in *mig-15(rh148)*. Thus, *mig-15* loss of function caused reversal of both AQR and PQR direction of migration. Reversal of AQR direction of migration was also not observed in Wnt signaling mutants *egl-20(mu39)*, *lin-17(e1456)*, or *bar-1(ga80)* (Figure 7).

Anterior migration of PQR in *mig-15* mutants was likely due to failure of *mab-5* expression in QL descendants as shown above. That AQR migrated posteriorly in some *mig-15(rh80)* animals suggested that *mab-5* might occasionally be expressed in QR descendants in *mig-15 (rh80)*. Indeed, posterior migration of AQR was dependent upon functional MAB-5, as the *mig-15(rh80); mab-5(e1239)* loss-of-function double mutant displayed no posteriorly-directed AQR neurons seen in *mig-15(rh80)* alone (Figures 8C and D). As expected, PQR was directed

to the anterior in *mab-5(e1239)* alone. These data suggest that MAB-5 function was required for the posterior migration of some AQR neurons in *mig-15(rh80)* and that *mab-5* might be active in some QR descendants in *mig-15(rh80)*.

AQR and PQR fail in migration in *mig-15* mutants in a *mab-5*-independent manner

In addition to directional migration defects, AQR and PQR in *mig-15* mutants failed to migrate to their normal positions in the anterior and posterior (Figure 6). In *mig-15* mutants, posteriorly-directed PQRs often failed to reach the phasmid ganglion, and anteriorly-misdirected PQRs often failed to reach the left anterior deirid ganglion (the contralateral position of normal AQR migration), but stopped along the anterior migration route (Figures 6B, E and F). Furthermore, AQR neurons of *mig-15* mutants often failed in their migrations and stopped before reaching the right-side anterior deirid ganglion (Figures 6C, E, and F). AQR and PQR migration defects described above for *mig-15* were not observed in *bar-1(ga80)/β-catenin*, the presumptive null state of canonical Wnt signaling in Q cell migration (Figure 7). *egl-20(mu39)/Wnt* and *lin-17 (e1456)/Frizzled* displayed no AQR migration defects, but misdirected PQRs often failed to migrate completely (Figure 7). The nature of this defect in *egl-20* and *lin-17* is unclear, but *bar-1(ga80)* did not display PQR migration defects.

The failure of migration of AQR and PQR in *mig-15* mutants was not dependent upon *mab-5* activity, as *mig-15* doubles with *mab-5(e1239)* loss of function still showed AQR and misdirected PQR migration defects (Figure 8D). The constitutively-active *mab-5(e1751)* allele causes constitutive expression of *mab-5* in both QL and QR descendants (Salser and Kenyon, 1992). As expected, constitutively-active *mab-5(e1751)* caused both AQR and PQR to be directed to the posterior (Figure 8E) (Salser and Kenyon, 1992). In *mig-15(rh80); mab-5 (e1751)* doubles, both AQR and PQR were posteriorly directed but they often stopped along their posterior migration routes before reaching the phasmid ganglion, a defect rarely observed in *mab-5(e1751)* alone (Figure 8F). These results indicate that MIG-15 has a MAB-5-independent role in AQR and PQR migration.

mig-15 is expressed in the Q neuroblasts

To determine the expression pattern of *mig-15*, a transgene consisting of a 4-kb upstream promoter fragment of *mig-15* driving *gfp* was constructed (*mig-15::gfp*). This transcriptional *mig-15::gfp* transgene was expressed in hypodermis, muscle, pharynx, and neurons as previously described (data not shown) (Poinat et al., 2002). Additionally, *mig-15 promoter::gfp* expression was observed in both Q neuroblasts as well as in the lateral seam cells and P cells neighboring the Q cells (Figure 9).

mig-15 acts cell-autonomously in AQR and PQR migration

Mosaic analysis was used to determine if *mig-15* acts cell-autonomously (Herman, 1984; Yochem and Herman, 2005) (see Materials and Methods for details of the experimental design). Figure 10A shows the lineage relationships between marker cells used in this mosaic analysis (Sulston et al., 1983), and Supplemental Figures 1 and 2 show the loss profiles of each mosaic analyzed.

Mosaics that had lost *mig-15(+)* in AQR and/or PQR but retained *mig-15(+)* in other tissues were analyzed (Supplemental Figure 1). Forty seven mosaics had losses in the PQR lineage and displayed PQR direction and migration defects similar to *mig-15(rh80)* alone (Figure 10B and D). Twenty-five PQR(−) mosaics had detectable losses only in PQR as shown in Figure 10B, and 20/25 displayed PQR migration defects. Thirty three mosaics were identified that had lost *mig-15(+)* in AQR and displayed AQR migration defects similar to *mig-15(rh80)* alone (Figure 10C). Of mosaics that retained *mig-15(+)* in AQR or PQR, all but one had normal AQR or PQR migration (Supplemental Figure 1).

Next, mosaics that retained *mig-15(+)* in AQR and/or PQR but that had lost *mig-15(+)* in other tissues were analyzed (Supplemental Figure 2). Of 64 mosaics that retained *mig-15(+)* in PQR, 62 displayed normal PQR migration (Figure 10F). Of 61 mosaics that retained *mig-15(+)* in AQR, 60 showed normal AQR migration (Figure 10E).

In sum, this mosaic analysis is consistent with a cell autonomous role of *mig-15* in AQR and PQR migration. A caveat of this analysis is that V5L is a potential substrate cell of QL and is also the sister of QL. Non-autonomous function of *mig-15* in V5L could not be excluded by this mosaic analysis. However, QR and V4R, a potential substrate of QR migration, are derived from distant lineages (V4R is from AB.a whereas QR is from AB.p). Functions in these lineages were resolved by this mosaic analysis: 12 mosaics with losses in URXR, an AB.a derivative, but not AQR had normal AQR migration; and 22 mosaics with losses in AQR but not in URXR had defective AQR migration.

Discussion

Mutations in *mig-15* reduced the size of the initial Q cell protrusions during polarization but did not affect the direction of initial polarization. *mig-15* mutations also disrupted the later maintenance of Q cell polarity and migration of the cells in the anterior (QR) and posterior (QL) directions. Later, after the Q cells have divided, *mig-15* affected the ability of the Q descendants AQR and PQR to migrate along their routes. Thus, MIG-15 might be required for robust Q cell polarization, maintenance of Q cell polarity, Q cell migration, and migration of the Q cell descendant neurons.

MIG-15 affects Q cell polarization, maintenance of polarity, and migration

Strong loss-of-function of *mig-15* resulted in shortened and less-robust Q cell protrusions, with QL and QR equally affected. Interestingly, the hypomorphic *mig-15(rh148)* did not strongly affect initial polarization. Possibly, robust protrusion requires less *mig*-15 activity than does maintenance of polarity and migration, and the hypomorphic *mig-15(rh148)* might provide enough activity for proper polarization. *mig-15(rh148)* is a missense mutation in a conserved residue of the ATP-binding pocket of the kinase domain (Shakir et al., 2006). An alternate explanation is that the kinase activity of MIG-15, which might be specifically disrupted in *mig-15(rh148)*, is not required for initial Q cell polarization.

Both *mig-15(rh80)* and *mig-15(rh148)* affected maintenance of Q cell polarity and Q cell migration. These might be distinct processes, as *mig-15(rh148)* had little effect on initial Q cell polarization but had a later effect on maintenance of Q cell polarity and migration.

Failure of QL migration in *mig-15* might perturb *mab-5* expression

In *mig-15(rh148)* mutants, *mab-5* often failed to be expressed in QL descendants, an effect also seen with the *qid-7/qid-8* alleles of *mig-15* (Ch'ng et al., 2003). Furthermore, the QL descendant PQR often migrated anteriorly instead of posteriorly in *mig-15* mutants, an expected effect of failure to express *mab-5* in these cells. The penetrance of failure of *mab-5* expression in *mig-15(rh148)* (35%; see Results) is in line with PQR direction of migration defects in *mig-15(rh148)* (39%; Figure 6E). It is possible that MIG-15 acts in this Wnt signaling pathway in addition to affecting early Q cell polarization and migration. Alternatively, the failure of QL to migrate posteriorly might result in a failure of some QL descendants to receive this Wnt signal. The observations that some AQR (QR descendants) migrated posteriorly in *mig-15(rh80)* and that this posterior migration was dependent upon functional MAB-5 supports the latter model. If MIG-15 acts in Wnt signaling and MAB-5 expression, MAB-5-dependent posterior migration of AQR would not be expected. Possibly, due to a failure in initial anterior migration of QR in *mig-15(rh80)*, QR responds to the posterior Wnt signal and activates

MAB-5. The lower penetrance of posterior migration of AQR (6%; Figure 6F) compared to QR migration defects (45%; Figure 4G) could be explained by the previous observation that QR is inherently less responsive than QL to the Wnt signal that controls *mab-5* expression (Whangbo and Kenyon, 1999).

MIG-15 is required for Q descendant migration

In *mig-15* mutants, AQR and PQR often failed to migrate to their normal final positions. Q descendant migration defects were independent of MAB-5, as migration defects were observed in *mab-5* loss-of-function and gain-of-function doubles with *mig-15*. MIG-15 might be required for the ability of AQR and PQR neurons to migrate along their normal routes. MIG-15 might control the speed of AQR and PQR migration or might control migration decisions at specific choicepoints along their migration routes. Further studies of MIG-15 in AQR and PQR migration will address these hypotheses.

mig-15 acts cell-autonomously in Q descendant migration

Loss of *mig-15* in the PQR lineage resulted in both PQR direction and migration defects and loss in the AQR lineage results in AQR migration defects, despite retention of *mig-15(+)* in other tissues. Conversely, retention of *mig-15* activity in AQR or PQR lineages resulted in normal migration of these neurons despite loss in other tissues. The EGL-20 Wnt signal that controls *mab-5* expression emanates from the K, F, U, and B blast cells as well as from the anal muscle muAnal and the P9/P10 ectoblasts (Whangbo and Kenyon, 1999). QL, derived from AB.pla, is separated in lineage from these cells, derived from AB.pr and AB.plp. While EGL-20-secreting cells were not specifically assayed in this mosaic analysis, the consistency of the data suggesting cell autonomy, the numbers of mosaics analyzed, and the wide lineage separation of QL and EGL-20-secreting cells suggests that MIG-15 is not required in these cells. A non-autonomous role of MIG-15 in V5L for QL migration could not be distinguished due to the fact that they are sister cells, but a non-autonomous role of V4R in QR migration could be excluded by this analysis (QR is an AB.p derivative and V4R is an AB.a derivative). While AQR and PQR migration was assayed in this mosaic analysis, it is likely that MIG-15 acts autonomously in initial Q cell polarization and migration, as anterior misdirection of PQR was cell-autonomous and likely dependent upon initial QL polarization and migration. In sum, this mosaic analysis is consistent with a cell-autonomous role of *mig-15* in initial Q cell polarization and migration and Q descendant migration.

MIG-15 and cell polarization and migration

These results indicate that MIG-15 is required for robust Q cell polarization, maintenance of Q cell polarity, and Q cell migration. The cellular mechanisms underlying these events could be the same, although *mig-15(rh148)* affects maintenance and migration without affecting polarity, suggesting the mechanisms might be distinct. In cultured cells, NIK kinase activity drives lamellipodial extension dependent upon the ERM class of actin modulatory molecules (Baumgartner et al., 2006), consistent with failure of *mig-15* mutants to extend robust lamellipodial protrusions during polarization. NIK kinases also physically and functionally interact with β1 integrin (Becker et al., 2000; Poinat et al., 2002). Possibly, failure to maintain Q cell polarity in *mig-15* mutants is due to defects in adhesion mediated by integrin. NIK kinases are also involved in nuclear migration (Houalla et al., 2005), which could explain the failure of the Q cell bodies to migrate over the V cells, although this could also be due to a failure in initial polarization or maintenance of polarity. Further studies of MIG-15 in polarization and migration will be guided by these hypotheses.

Materials and Methods

Genetic Methods

All experiments were performed at 20°C using standard techniques (Brenner, 1974; Sulston and Hodgkin, 1988). The following mutations and transgenic constructs were used: X: *bar-1 (ga80), qid-7(mu327), qid-8(mu342), mig-15(rh148* and *rh80)*; I: *lin-17(e1456), lqIs40 [Pgcy-32::gfp]*; II: *muIs16*; III: *gmIs5[mab-5::gfp], mab-5(e1239* and *e1751)*; IV: *lqIs3 [osm-6::gfp]*. The chromosomal locations of *lqIs80[scm promoter::gfp::caax]* and *lqIs58 [Pgcy-32::cfp]* were not determined. *Pmig-15::gfp*, *Pgcy-32::yfp*, and *mig-15(+)* were extrachromosomal arrays. Extrachromosomal arrays were generated by germ line microinjection and integrated into the genome by standard techniques (Mello and Fire, 1995).

Synchronization of L1 larvae to visualize Q cell polarization—Methods described previously to synchronize larval development were used (Honigberg and Kenyon, 2000). Adults and larvae were washed from a plate with M9 buffer. Eggs adhered to the agarose and were not removed. Newly-hatched L1 larvae were washed from the plate at 30 minute intervals, placed on a fresh NGM plate with a bacterial lawn, and allowed to develop for given times: imaged immediately (0–0.5h), 1–2.5h, 3–3.5h, 4–4.5h, and 5.5–6h (for *mig-15(rh80)*). In the case of egg-laying-defective genotypes, eggs were isolated from gravid adults by bleach treatment (Sulston and Hodgkin, 1988).

Epifluorescence microscopy and visualization of Q cell polarization and migration—Animals were analyzed by epifluorescence microscopy for GFP, YFP, or CFP using a Leica DMR compound microscope. Images were captured using Openlab software and a Qimaging Retiga EXi camera. For Q cell imaging, a z-series of images of the Q cells was captured, and images were subjected to nearest-neighbor deconvolution (Openlab).

Scoring and analysis of AQR and PQR migration defects—The final positions of AQR and PQR were scored in L4 larvae and young adult worms. The position of each neuron was given a value of 1–5, depending on the anterior-posterior position of the neuron: a value of 1 was the normal position of AQR in the anterior deirid ganglion; 2 was posterior to the anterior deirid to approximately half the distance to the vulva; 3 was around the vulva (half the distance from the vulva to the anterior deirid and from the vulva to the post-deirid); 4 was the post-deirid to the anus; and 5 was posterior to the anus, the normal position of PQR in the phasmid ganglion. A position of 4, around the post-deirid, is the position of Q cell birth. Thus, some cells with a score of 4 had not migrated from the Q cell birthplaces. PQR neurons with scores of 1 to 3 had reversed direction and migrated anteriorly instead of posteriorly. AQR neurons with a score of 5 had reversed direction of migration and migrated posteriorly instead of anteriorly. These coordinates correspond to the following landmarks in the L1 larva: 1 = anterior to the V1.a/p cells; 2 = near the V1.a/p and V2.a/p cells; 3 = near the V3.a/p and V4.a/p cells; 4 = near the V4.a/p, V5.a/p, and V6.a/p cells (Q cells are born between V4 and V5); and 5 = posterior to the anus.

***mig-15, gcy-32,* and *scm::gfp::caax* transgenes—**The sequences of all plasmids and primers used in this work are available upon request. All coding regions amplified by polymerase chain reaction (PCR) were sequenced to ensure that no mutations had been introduced by PCR. All regions were amplified from N2 genomic DNA unless otherwise noted. The entire *mig-15(+)* gene included the entire *mig-15* coding region plus 4-kb of upstream promoter sequence. The *mig-15* promoter included 4-kb of DNA upstream of the *mig-15* coding region and was placed upstream of the *gfp* coding region in vector pPD95.77 (kindly provided by A. Fire). The *scm::gfp::caax* transgene was constructed using the seam cell marker (*scm*) plasmid pRT1 (Terns et al., 1997). The *lacZ* coding region of pRT1 was replaced by *gfp* coding

region with the C-terminal CAAX prenylation domain coding region from *ced-10 Rac* at the 3' end (Reddien and Horvitz, 2000). *scm::gfp::caax* drove expression of membrane-associated, prenylated GFP in the lateral seam cells and in the Q neuroblasts. A similar construct was used previously to image Q cell development (Williams, 2002). The *gcy::32::gfp* transgene *adEx1295* (Yu et al., 1997) was integrated into the genome to generate *lqIs40*. For the *Pgcy-32::yfp* and *Pgcy-32::cfp* constructs, the *gcy-32* promoter was generated by PCR and placed upstream of the *yfp* and *cfp* coding regions (courtesy of A. Fire).

qid-7* and *qid-8* complementation tests and sequencing—mig-15(rh148)* and *mig-15 (rh80)* males harboring the rescuing *mig-15(+)* transgene were mated to *qid-7* and *qid-8* hermaphrodites, and some *trans*-heterozygous cross progeny displayed the Unc Dpy phenotype indicating failure to complement. The *mig-15* coding regions from *qid-7(mu327)* and *qid-8 (mu342)* animals were amplified by PCR and sequenced. Nucleotide lesions were found associated with both as described in Figure 1 and were confirmed with second-strand sequencing.

Mosaic Analysis—An extrachromosomal array containing the wild-type *mig-15(+)* coding region rescued the gross morphological phenotype (Unc Dpy) as well as AQR and PQR migration defects of *mig-15(rh80)* (Figures 10C and D). Included in this extrachromosomal array was a *gcy-32::yfp* transgene, which drove the expression of yellow fluorescent protein (YFP) in AQR, PQR, and the two bilateral URX neurons. This extrachromosomal array was spontaneously lost during mitotic divisions, resulting in mosaic animals in which some cells harbored the *mig-15(+)* transgene and other did not. AQR, PQR, and URX neurons with the transgene expressed YFP whereas those that lost the transgene did not. In these studies, approximately 10% of animals harboring this extrachromosomal array displayed mosaicism in AQR, PQR and the URX neurons, and animals with multiple losses were observed and analyzed.

A strain was constructed including *mig-15(rh80)*, the rescuing *mig-15(+) gcy-32::yfp* extrachromosomal array, and a stable, integrated *gcy-32::cfp* transgene, which drove expression of cyan fluorescent protein (CFP) in AQR, PQR, and the two URX neurons and which was used to report AQR and PQR position (see Figure 10B).

To identify mosaics with losses in AQR and PQR, animals with a wildtype gross morphological phenotype (non-Dpy non-Unc) were screened for those that lacked YFP expression in AQR and/or PQR. These animals retained *mig-15(+)* function in tissues underlying the Dpy and Unc defects of *mig-15* mutants, and many of these mosaics also maintained *mig-15(+)* in AQR, PQR, or the URX L/R neurons as judged by YFP fluorescence (Supplemental Figure 1).

To identify mosaics that retained *mig-15(+)* in AQR or PQR, animals with the *mig-15* gross morphological phenotype (Unc and Dpy) were screened for those with YFP expression in AQR and/or PQR. These animals had lost *mig-15(+)* in tissues underlying the Dpy Unc phenotype but retained *mig-15(+)* in AQR and PQR. In 44/70 of these animals, no loss could be detected in the AQR, PQR and URX L/R neurons, suggesting that the cellular focus of the Dpy Unc phenotype of *mig-15* was in the P lineage and not the AB lineage. Many of these also retained *mig-15(+)* in AQR or PQR and the URX neurons (Supplemental Figure 2).

Supplementary Material

Refer to Web version on PubMed Central for supplementary material.

Acknowledgements

We wish to thank the Caenorhabditis Genetics Center, sponsored by the NIH National Institute of Research Resources, and the *C. elegans* Gene Knockout Consortium (Bob Barstead, Gary Moulder, Mark Edgley, Don Moerman) for strains, J. Rothman for pRT1[*scm::lacZ*], E. Struckhoff for technical assistance, M. Herman for critical reading of the manuscript, and members of the Lundquist lab for helpful discussions. This work was supported by NIH grant NS40945 and NSF grant IOS93192 to E.A.L, and NIH grant P20 RR016475 from the INBRE Program of the National Center for Research Resources (J. Hunt, P.I.).

Literature Cited

Baumgartner M, Sillman AL, Blackwood EM, Srivastava J, Madson N, Schilling JW, Wright JH, Barber DL. The Nck-interacting kinase phosphorylates ERM proteins for formation of lamellipodium by growth factors. Proc Natl Acad Sci U S A 2006;103:13391–6. [PubMed: 16938849]

Becker E, Huynh-Do U, Holland S, Pawson T, Daniel TO, Skolnik EY. Nck-interacting Ste20 kinase couples Eph receptors to c-Jun N-terminal kinase and integrin activation. Mol Cell Biol 2000;20:1537–45. [PubMed: 10669731]

Brenner S. The genetics of *Caenorhabditis elegans*. Genetics 1974;77:71–94. [PubMed: 4366476]

Ch'ng Q, Williams L, Lie YS, Sym M, Whangbo J, Kenyon C. Identification of genes that regulate a left-right asymmetric neuronal migration in Caenorhabditis elegans. Genetics 2003;164:1355–67. [PubMed: 12930745]

Chalfie M, Sulston J. Developmental genetics of the mechanosensory neurons of Caenorhabditis elegans. Dev Biol 1981;82:358–70. [PubMed: 7227647]

Chalfie M, Thomson JN, Sulston JE. Induction of neuronal branching in Caenorhabditis elegans. Science 1983;221:61–3. [PubMed: 6857263]

Cowing D, Kenyon C. Correct Hox gene expression established independently of position in Caenorhabditis elegans. Nature 1996;382:353–6. [PubMed: 8684464]

Eisenmann DM. Wnt signaling. WormBook 2005:1–17. [PubMed: 18050402]

Eisenmann DM, Kim SK. Protruding vulva mutants identify novel loci and Wnt signaling factors that function during Caenorhabditis elegans vulva development. Genetics 2000;156:1097–116. [PubMed: 11063687]

Eisenmann DM, Maloof JN, Simske JS, Kenyon C, Kim SK. The beta-catenin homolog BAR-1 and LET-60 Ras coordinately regulate the Hox gene lin-39 during Caenorhabditis elegans vulval development. Development 1998;125:3667–80. [PubMed: 9716532]

Forrester WC, Kim C, Garriga G. The Caenorhabditis elegans Ror RTK CAM-1 inhibits EGL-20/Wnt signaling in cell migration. Genetics 2004;168:1951–62. [PubMed: 15371357]

Harris J, Honigberg L, Robinson N, Kenyon C. Neuronal cell migration in C. elegans: regulation of Hox gene expression and cell position. Development 1996;122:3117–31. [PubMed: 8898225]

Herman M. C. elegans POP-1/TCF functions in a canonical Wnt pathway that controls cell migration and in a noncanonical Wnt pathway that controls cell polarity. Development 2001;128:581–90. [PubMed: 11171341]

Herman, MA. Wnt signaling in C. elegans. In: Kühl, M., editor. Wnt signaling in Development. Landes Biosciences; Georgetown, TX: 2003. p. 187-212.

Herman RK. Analysis of genetic mosaics of the nematode Caneorhabditis elegans. Genetics 1984;108:165–80. [PubMed: 6434374]

Honigberg L, Kenyon C. Establishment of left/right asymmetry in neuroblast migration by UNC-40/DCC, UNC-73/Trio and DPY-19 proteins in C elegans. Development 2000;127:4655–68. [PubMed: 11023868]

Houalla T, Hien Vuong D, Ruan W, Suter B, Rao Y. The Ste20-like kinase misshapen functions together with Bicaudal-D and dynein in driving nuclear migration in the developing drosophila eye. Mech Dev 2005;122:97–108. [PubMed: 15582780]

Keino-Masu K, Masu M, Hinck L, Leonardo ED, Chan SS-Y, Culotti JG, Tessier-Lavigne M. *Deleted in Colorectal Cancer* (DCC) encodes a netrin receptor. Cell 1996;87:175–185. [PubMed: 8861902]

Kenyon C. A gene involved in the development of the posterior body region of C. elegans. Cell 1986;46:477–87. [PubMed: 3731276]

Korswagen HC, Herman MA, Clevers HC. Distinct beta-catenins mediate adhesion and signalling functions in C. elegans. Nature 2000;406:527–32. [PubMed: 10952315]

Maloof JN, Whangbo J, Harris JM, Jongeward GD, Kenyon C. A Wnt signaling pathway controls hox gene expression and neuroblast migration in C. elegans. Development 1999;126:37–49. [PubMed: 9834184]

Mello C, Fire A. DNA transformation. Methods Cell Biol 1995;48:451–82. [PubMed: 8531738]

Natarajan L, Witwer NE, Eisenmann DM. The divergent Caenorhabditis elegans beta-catenin proteins BAR-1, WRM-1 and HMP-2 make distinct protein interactions but retain functional redundancy in vivo. Genetics 2001;159:159–72. [PubMed: 11560894]

Poinat P, De Arcangelis A, Sookhareea S, Zhu X, Hedgecock EM, Labouesse M, Georges-Labouesse E. A conserved interaction between beta1 integrin/PAT-3 and Nck-interacting kinase/MIG-15 that mediates commissural axon navigation in C. elegans. Curr Biol 2002;12:622–31. [PubMed: 11967148]

Reddien PW, Horvitz HR. CED-2/CrkII and CED-10/Rac control phagocytosis and cell migration in Caenorhabditis elegans. Nat Cell Biol 2000;2:131–6. [PubMed: 10707082]

Salser SJ, Kenyon C. Activation of a C. elegans Antennapedia homologue in migrating cells controls their direction of migration. Nature 1992;355:255–8. [PubMed: 1346230]

Sawa H, Lobel L, Horvitz HR. The Caenorhabditis elegans gene lin-17, which is required for certain asymmetric cell divisions, encodes a putative seven-transmembrane protein similar to the Drosophila frizzled protein. Genes Dev 1996;10:2189–97. [PubMed: 8804313]

Shakir MA, Gill JS, Lundquist EA. Interactions of UNC-34 Enabled with Rac GTPases and the NIK kinase MIG-15 in Caenorhabditis elegans axon pathfinding and neuronal migration. Genetics 2006;172:893–913. [PubMed: 16204220]

Steven R, Kubiseski TJ, Zheng H, Kulkarni S, Mancillas J, Ruiz Morales A, Hogue CWV, Pawson T, Culotti J. UNC-73 activates the Rac GTPase and is required for cell and growth cone migrations in *C. elegans*. Cell 1998;92:785–795. [PubMed: 9529254]

Su YC, Han J, Xu S, Cobb M, Skolnik EY. NIK is a new Ste20-related kinase that binds NCK and MEKK1 and activates the SAPK/JNK cascade via a conserved regulatory domain. EMBO J 1997;16:1279–90. [PubMed: 9135144]

Su YC, Maurel-Zaffran C, Treisman JE, Skolnik EY. The Ste20 kinase misshapen regulates both photoreceptor axon targeting and dorsal closure, acting downstream of distinct signals. Mol Cell Biol 2000;20:4736–44. [PubMed: 10848599]

Su YC, Treisman JE, Skolnik EY. The Drosophila Ste20-related kinase misshapen is required for embryonic dorsal closure and acts through a JNK MAPK module on an evolutionarily conserved signaling pathway. Genes Dev 1998;12:2371–80. [PubMed: 9694801]

Sulston, J.; Hodgkin, J. Methods. In: Wood, WB., editor. The Nematode *Caenorhabditis elegans*. Cold Spring Harbor Laboratory Press; Cold Spring Harbor, New York: 1988. p. 587-606.

Sulston JE, Horvitz HR. Post-embryonic cell lineages of the nematode, Caenorhabditis elegans. Dev Biol 1977;56:110–56. [PubMed: 838129]

Sulston JE, Schierenberg E, White JG, Thomson JN. The embryonic cell lineage of the nematode *Caenorhabditis elegans*. Dev Biol 1983;100:64–119. [PubMed: 6684600]

Sym M, Robinson N, Kenyon C. MIG-13 positions migrating cells along the anteroposterior body axis of C. elegans. Cell 1999;98:25–36. [PubMed: 10412978]

Terns RM, Kroll-Conner P, Zhu J, Chung S, Rothman JH. A deficiency screen for zygotic loci required for establishment and patterning of the epidermis in Caenorhabditis elegans. Genetics 1997;146:185–206. [PubMed: 9136010]

Whangbo J, Kenyon C. A Wnt signaling system that specifies two patterns of cell migration in C. elegans. Mol Cell 1999;4:851–8. [PubMed: 10619031]

White JG, Southgate E, Thomson JN, Brenner S. The structure of the nervous system of the nematode *Caenorhabditis elegans*. Philos Trans R Soc Lond 1986;314:1–340.

Williams, L. PhD thesis. University of California-San Francisco; 2002. A genetic analysis of the left-right asymmetric polarizations and migrations of the Q neuroblasts in C. elegans.

Xue Y, Wang X, Li Z, Gotoh N, Chapman D, Skolnik EY. Mesodermal patterning defect in mice lacking the Ste20 NCK interacting kinase (NIK). Development 2001;128:1559–72. [PubMed: 11290295]

Yochem J, Herman RK. Genetic mosaics. WormBook 2005:1–6.

Yu S, Avery L, Baude E, Garbers DL. Guanylyl cyclase expression in specific sensory neurons: a new family of chemosensory receptors. Proc Natl Acad Sci U S A 1997;94:3384–7. [PubMed: 9096403]

Zinovyeva AY, Yamamoto Y, Sawa H, Forrester WC. Complex Network of Wnt Signaling Regulates Neuronal Migrations During Caenorhabditis elegans Development. Genetics 2008;179:1357–71. [PubMed: 18622031]

Figure 1. The MIG-15 NIK kinase

MIG-15 contains a STE20 class serine/threonine kinase domain, a proline rich domain (PRD), and a citron/NIK homology (CNH) domain. The effects of the *mu327*, *rh148*, *mu342*, *rh326*, and *rh80* mutations are shown. *qid-7(mu327)* was a G to A missense mutation at position 89 in the *mig-15* open reading frame, resulting in glycine 30 to glutamic acid change. *qid-8 (mu342)* was a G to A missense mutation at position 667, resulting in glutamic acid 223 to lysine change.

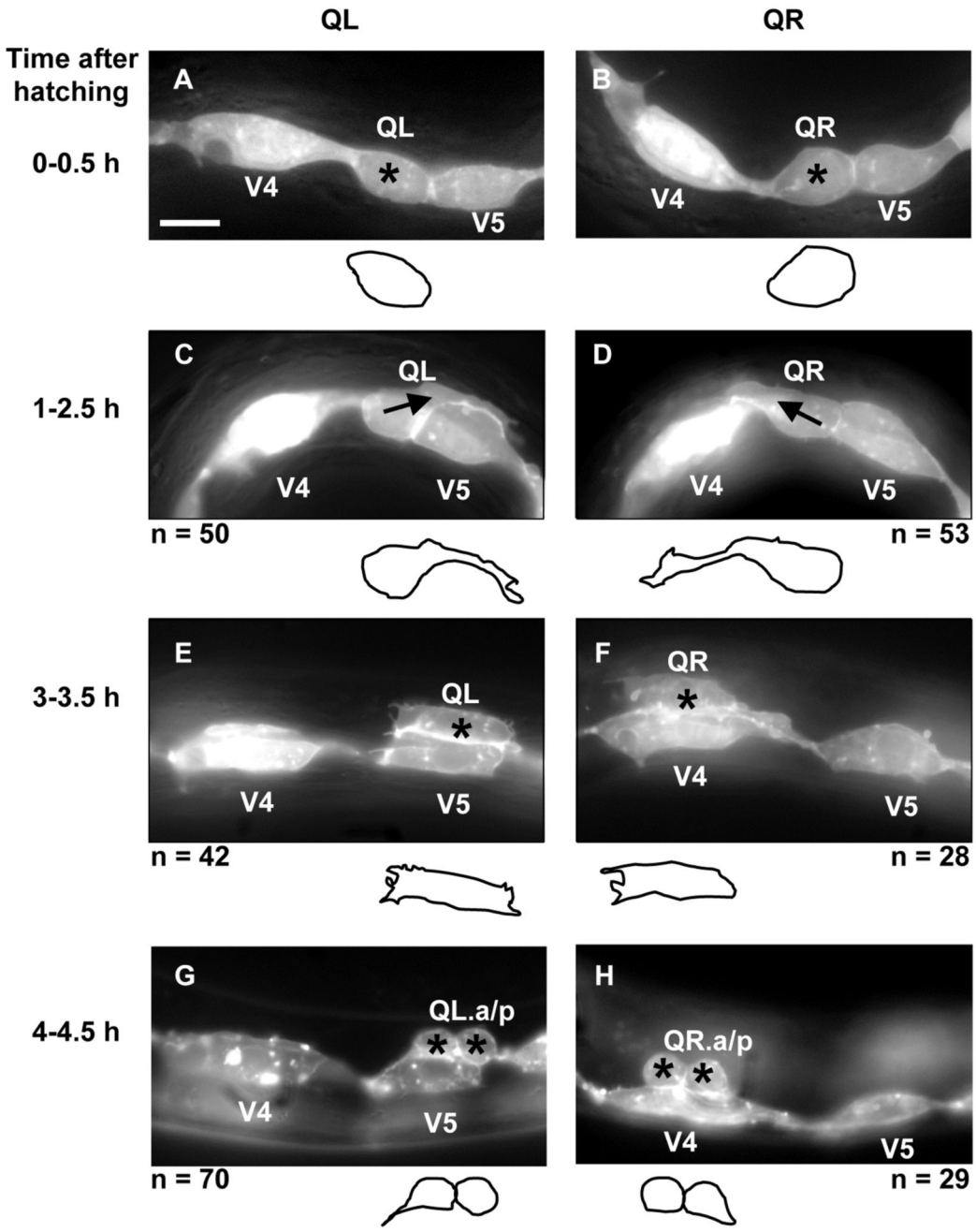

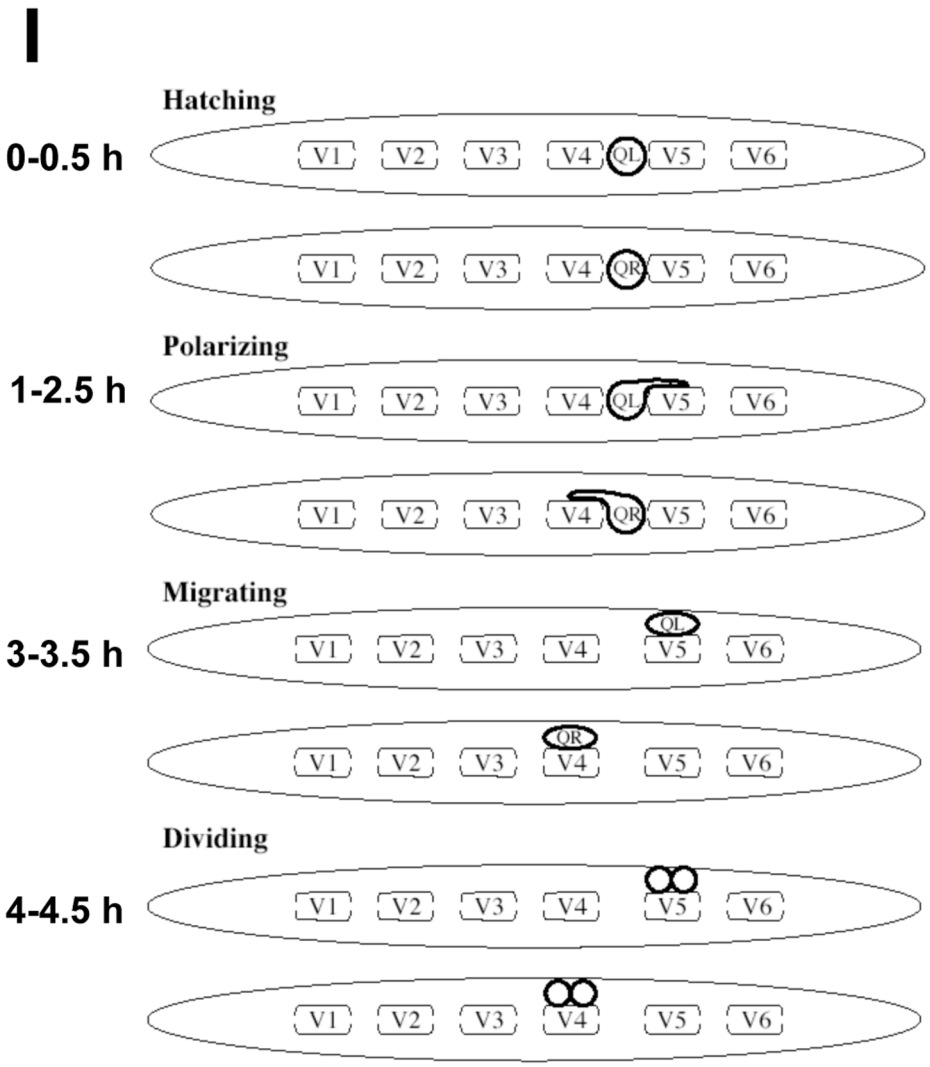

Figure 2. Q neuroblast polarization and migration

(A–H) are panels of epifluorescent micrographs of Q neuroblasts of L1 larvae at given timepoints after hatching expressing the *scm::gfp::caax* marker in the Q cells and the lateral seam cells (V cells). Tracings of the boundaries of the Q neuroblasts in each micrograph are located below each panel. For each time point, the QL neuroblast is found on the left (A,C,E,G) and the QR neuroblast is found on the right (B,D,F,H). The scale bar in (A) represents 5μm for (A–H). (A–B) Unpolarized Q neuroblasts visualized 0–0.5 h after hatching. Asterisks mark the position of the Q neuroblasts. (C–D) Polarization of the Q neuroblasts visualized 1–2.5 h after hatching. QL sent a process posteriorly over the V5L seam cell. QR sent a process anteriorly over the V4R seam cell. Arrows indicate the direction of polarization of the Q neuroblasts. (E–F) Migration of the Q neuroblasts visualized 3–3.5 h after hatching. QL migrated posteriorly over the V5L seam cell. QR migrated anteriorly over the V4R seam cell. (G–H) Division of the Q neuroblasts visualized 4–4.5 h after hatching. QL divided over the V5L seam cell to produce QL.a and QL.p. QR divided over the V4R seam cell to produce QR.a and QR.p. Asterisks mark the position of the Q neuroblast daughters. (I) A schematic diagram demonstrating the polarization, migration, and division patterns of the Q neuroblasts.

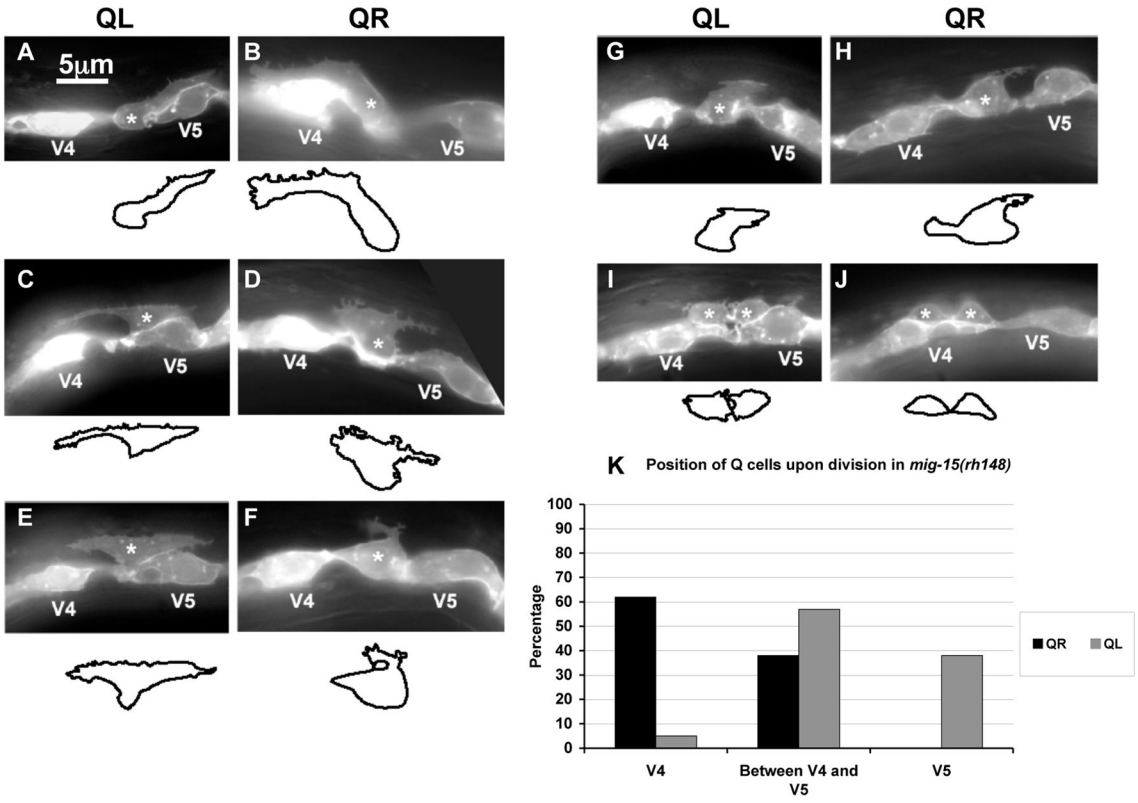

Figure 3. *mig-15* NIK kinase hypomorphic mutation affects the polarizations and migrations of the Q neuroblasts

(A–J) are panels of epifluorescent micrographs of Q neuroblasts of L1 larvae in *mig-15 (rh148)* mutants with *scm::gfp::caax* expression. Asterisks mark the position of the Q neuroblast at 3–3.5 h after hatching (A–H) or Q neuroblast descendants at 4–4.5 h after hatching (I–J). Tracings of the Q neuroblasts found in each micrograph are located below each panel. The scale bar in (A) represents 5μm for (A–J). (A) A QL neuroblast polarized normally over the V5L seam cell. (B) A QR neuroblast polarized normally over the V4R seam cell. (C) A QL neuroblast failed to maintain proper posterior polarization, and sent a protrusion to the anterior. (D) A QR neuroblast failed to maintain proper anterior polarization, and sent a protrusion to the posterior. (E) A QL neuroblast sent protrusions to both the anterior and posterior. (F) A QR neuroblast was not strongly polarized in either direction and sent a small, anteriorly-directed protrusion from the posterior of the cell. (G) A QL neuroblast was not strongly polarized in either the anterior or posterior direction, although maintained slight posterior polarization. (H) A QR neuroblast was not strongly polarized in either the anterior or posterior direction and sent a small protrusion posteriorly. (I) A QL neuroblast divided between the V4L and V5L seam cells. (J) A QR neuroblast divided over the V4R seam but was not atop the V4R seam cell. (K) Quantitation of the position of the QL and QR neuroblasts upon division (4–4.5 h after hatching) in *mig-15(rh148)* mutants. Position with respect to the V4 and V5 seam cells is the X axis, and the percentage of Q neuroblast daughters found at those positions is the Y axis. For QL divisions, 37 animals were scored. For QR divisions, 26 animals were scored.

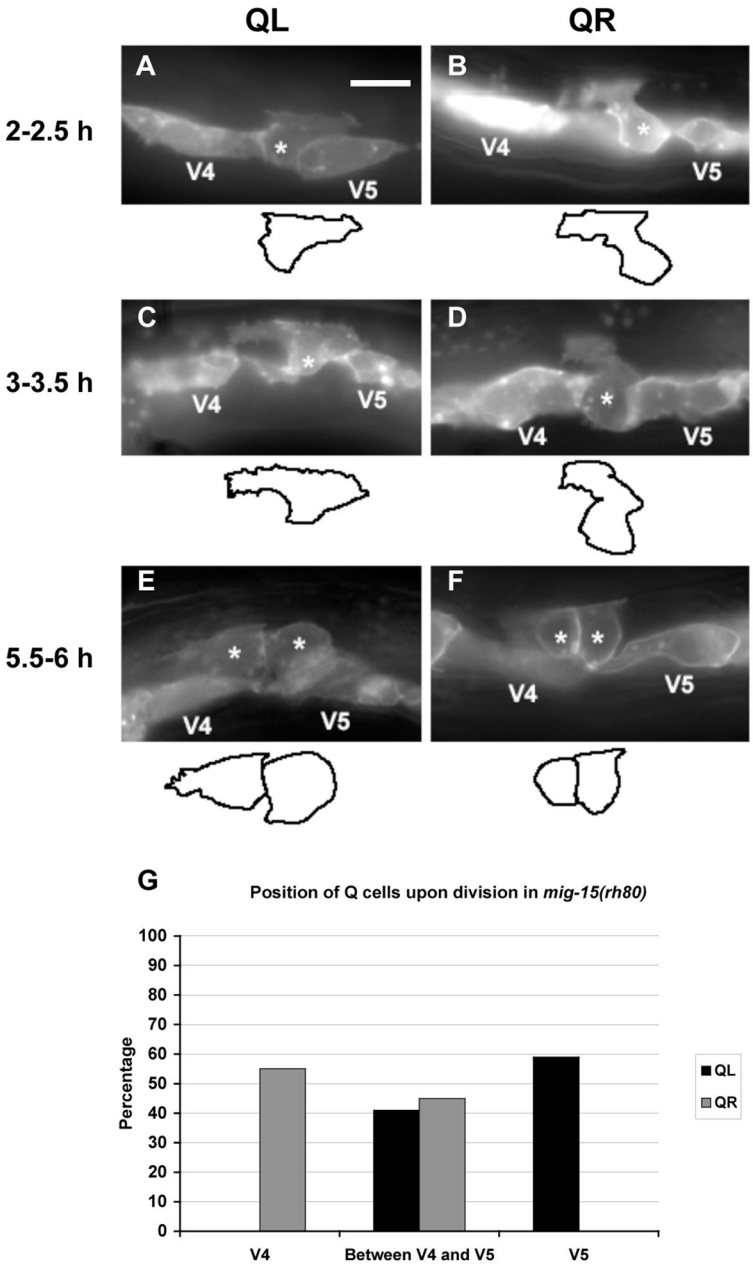

Figure 4. *mig-15* NIK kinase strong loss-of-function mutation affects the polarizations and migrations of the Q neuroblasts

(A–F) are panels of epifluorescent micrographs of Q neuroblasts of L1 larvae in *mig-15 (rh80)* mutants with *scm::gfp::caax* expression. Asterisks mark the position of the Q neuroblast at 2–2.5 h after hatching (A–B) and 3–3.5 h after hatching (C–D) or Q neuroblast descendants at 5.5–6 h after hatching (E–F). Tracings of the Q neuroblasts found in each micrograph are located below each panel. The scale bar in (A) represents 5μm for (A–F). (A) A QL neuroblast polarized posteriorly over the V5L seam cell, but did not extend its protrusion nearly as far as in wild type. (B) A QR neuroblast polarized anteriorly over the V4R seam cell, but did not extend its protrusion nearly as far as in wild type. (C) A QL neuroblast sent protrusions in both anterior and posterior directions. (D) A QR neuroblast did not polarize strongly in either direction, although it sent a small protrusion anteriorly. (E) A QL neuroblast divided between

the V4L and V5L seam cells. (F) A QR neuroblast divided between the V4R and V5R seam cells. (G) Quantitation of the position of the QL and QR neuroblasts upon division (5.5–6 h after hatching) in *mig-15(rh80)* mutants. The graph is organized as described in Figure 3K. For QL divisions, 41 animals were scored. For QR divisions, 38 animals were scored.

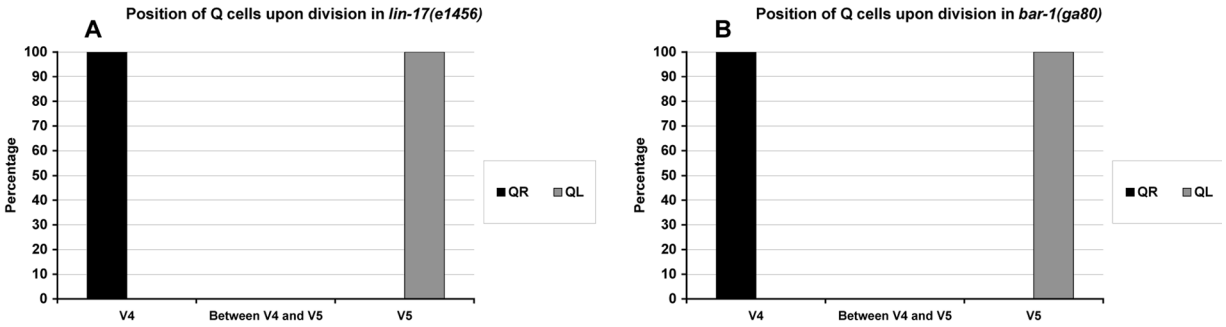

Figure 5. Canonical Wnt signaling does not affect the migrations of the Q neuroblasts

The graphs are organized as described in Figure 3K. (A) Quantitation of the position of the QL and QR neuroblasts upon division (4–4.5 h after hatching) in *lin-17(e1456)* mutants. For QL divisions, 28 animals were scored. For QR divisions, 16 animals were scored. (B) Quantitation of the position of the QL and QR neuroblasts upon division (4–4.5 h after hatching) in *bar-1 (ga80)* mutants. For QL divisions, 37 animals were scored. For QR divisions, 17 animals were scored.

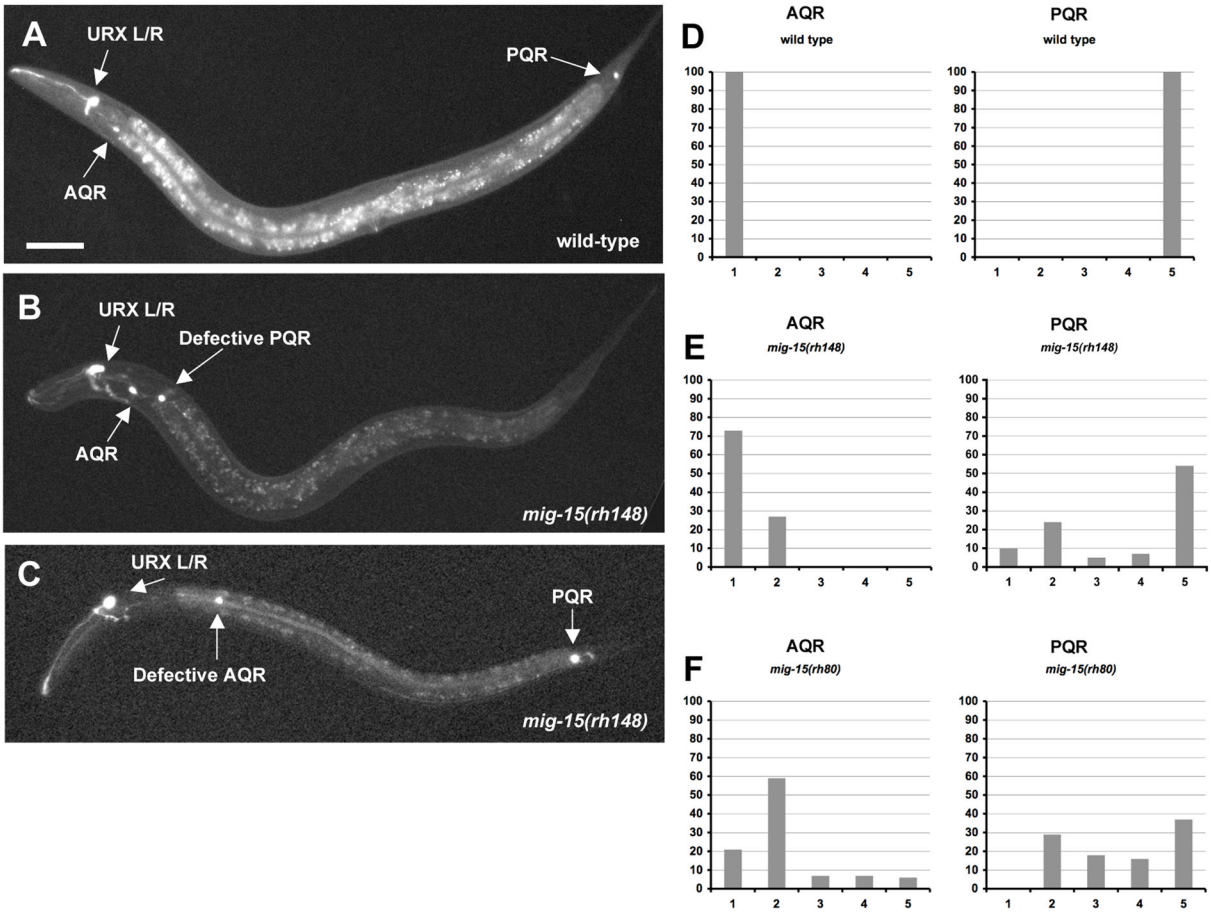

Figure 6. The Q neuroblast descendants AQR and PQR have direction of migration defects and fail to migrate in *mig-15* NIK kinase hypomorphic mutants

(A–C) are panels of epifluorescent micrographs of AQR and PQR neurons of L4 larvae with *gcy-32::gfp* expression. The scale bar in (A) represents 50μm for (A–C). (A) A wild-type animal with AQR located near the anterior deirid ganglion and PQR near the phasmid ganglion. (B) A *mig-15(rh148)* hypomorphic mutant with AQR located in its normal position. PQR migrated anteriorly, but failed to migrate to the same anterior-posterior position as AQR. (C) A *mig-15(rh148)* mutant with PQR located in its normal position. AQR migrated anteriorly, but failed to migrate completely to reside near the anterior deirid ganglion. (D–F) Quantitation of the final migratory positions of AQR and PQR. Anterior-posterior position of AQR and PQR is the X axis (see Materials and Methods section for description of the classifications of the anterior-posterior positions), and the percentage of AQR and PQR found at those positions in the Y axis. In each case, 100 animals were scored.

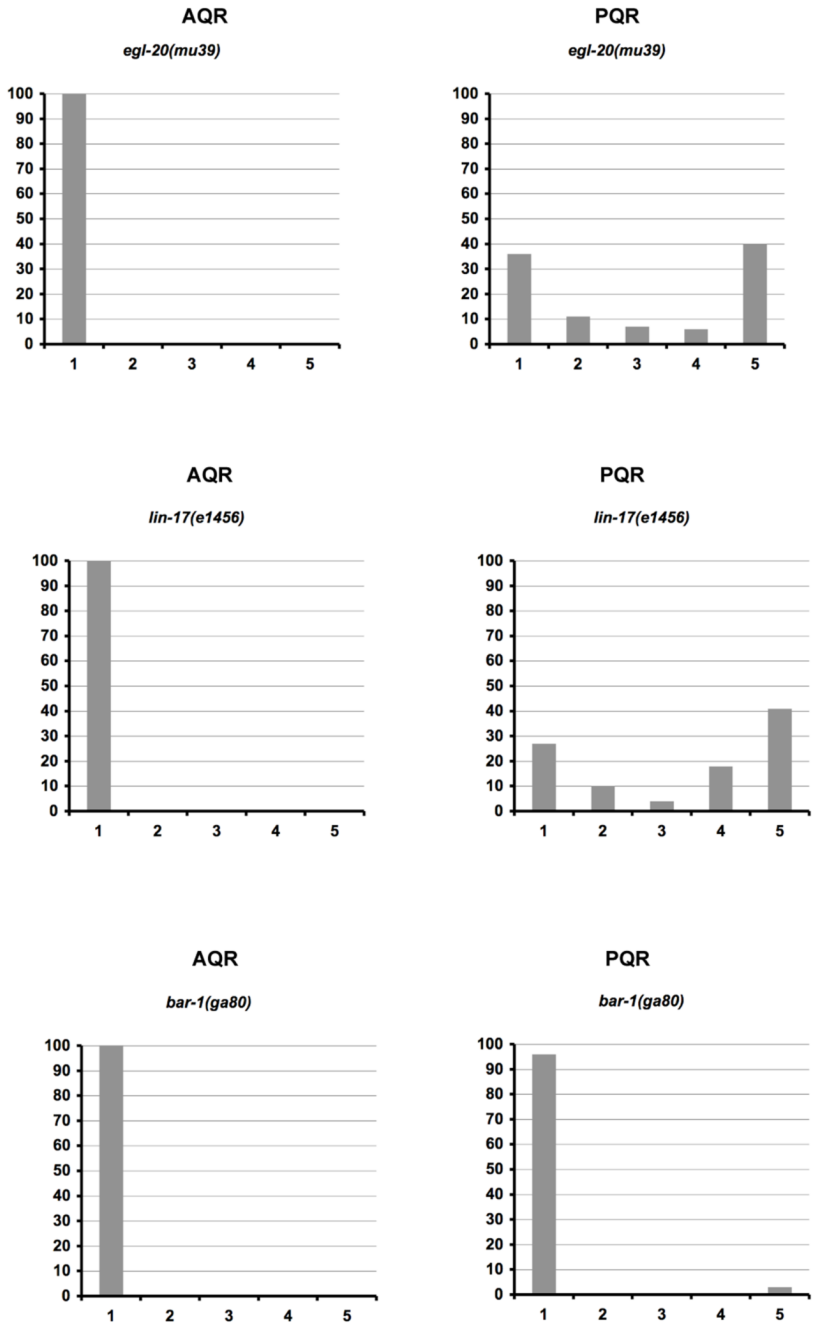

Figure 7. The PQR neuron has direction of migration defects and fails to migrate in canonical Wnt signaling mutants

Quantitation of the final migratory positions of AQR and PQR. The graphs are organized as described in Figure 6D–F. For *egl-20(mu39)* and *lin-17(e1456)*, 100 animals were scored. For *bar-1(ga80)*, 200 animals were scored.

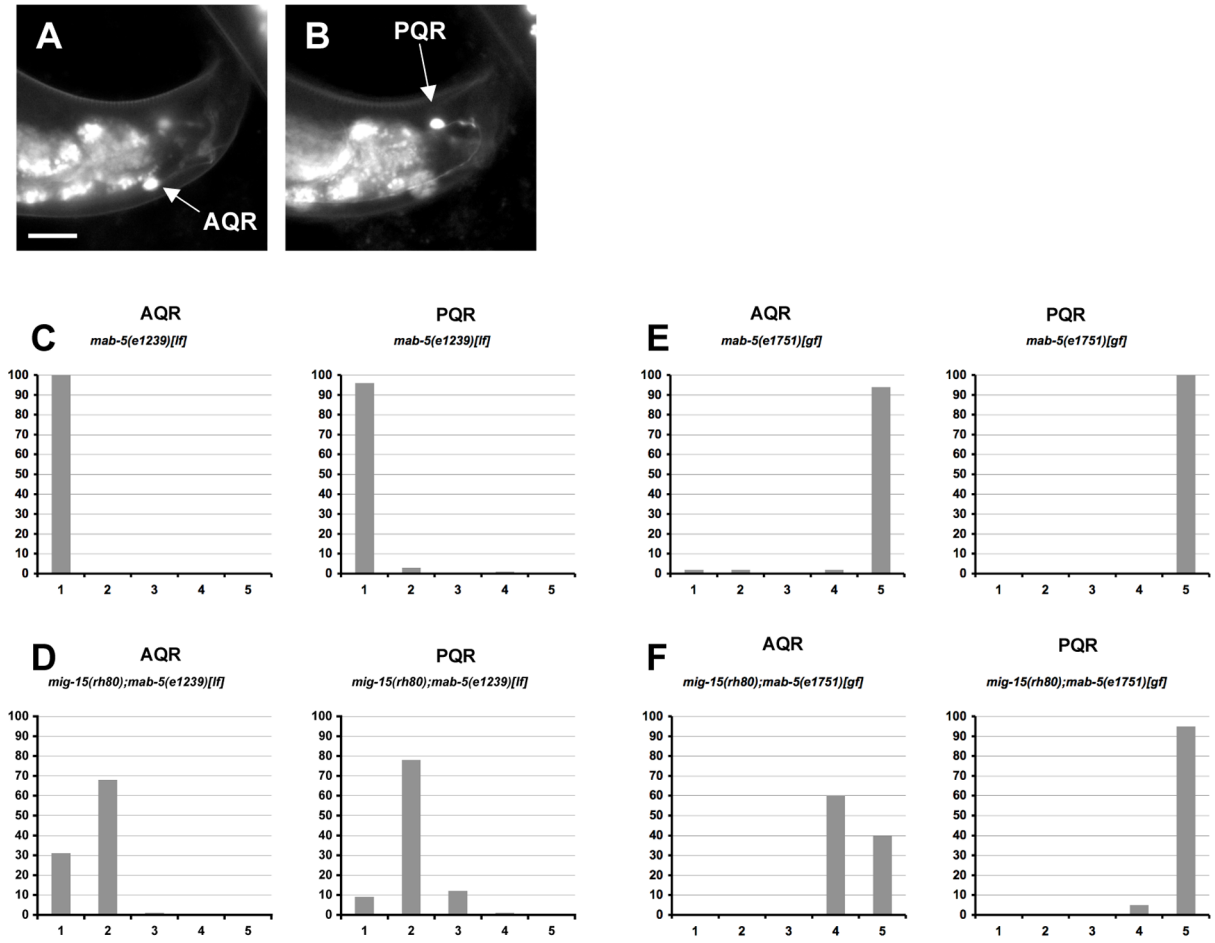

Figure 8. The AQR/PQR direction of migration defects seen in *mig-15* NIK kinase hypomorphic mutants are dependent on MAB-5, whereas the failure to migrate defects are independent of MAB-5

(A–B) are panels of epifluorescent micrographs of AQR and PQR neurons of a young adult in a *mig-15(rh80)* mutant with *gcy-32::gfp* expression. An AQR neuron (A) reversed the direction of migration and migrated to the tail of the animal near the PQR neuron (B). The scale bar in (A) represents 10μm for (A–B). (C–F) Quantitation of the final migratory positions of AQR and PQR. The graphs are organized as described in Figure 6D–F. *mab-5(e1239)[lf]* is a loss-of-function mutation, and *mab-5(e1751)[gf]* is a gain-of-function mutation. For each genotype, 100 animals were scored.

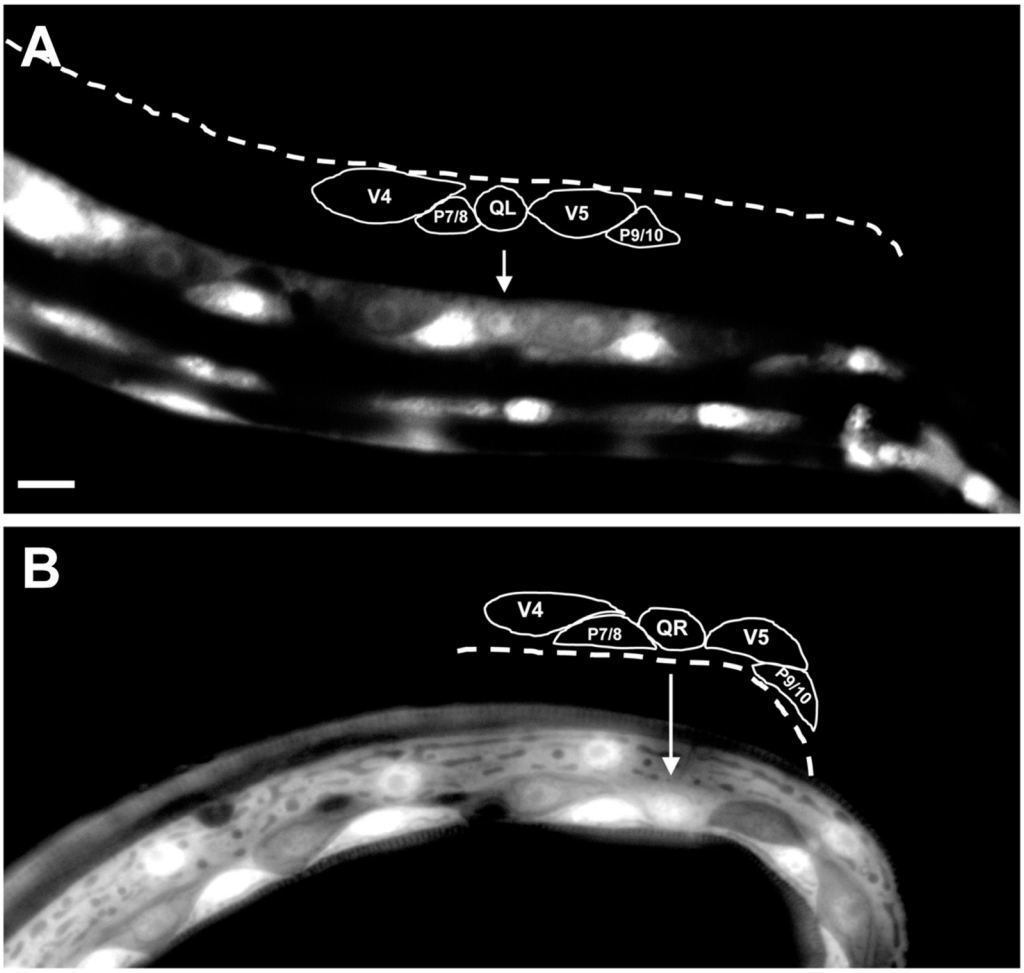

Figure 9. *mig-15* is expressed in the Q neuroblasts

Shown are epifluorescent micrographs of newly-hatched L1 larvae expressing the *mig-15::gfp* transcriptional promoter fusion. Tracings of the Q cells and the surrounding cells are shown above each micrograph. Arrows mark the positions of Q cells. (A) A left ventral-lateral view of an animal with *mig-15::gfp* expression in QL. The lateral seam cells (V cells) and P cells also express *mig-15::gfp*. (B) A right dorsal-lateral view of an animal with *mig-15::gfp* expression in QR. In this animal, the V5 seam cell lost *mig-15::gfp* and showed no fluorescence. The scale bar in (A) represents 5μm for (A–B).

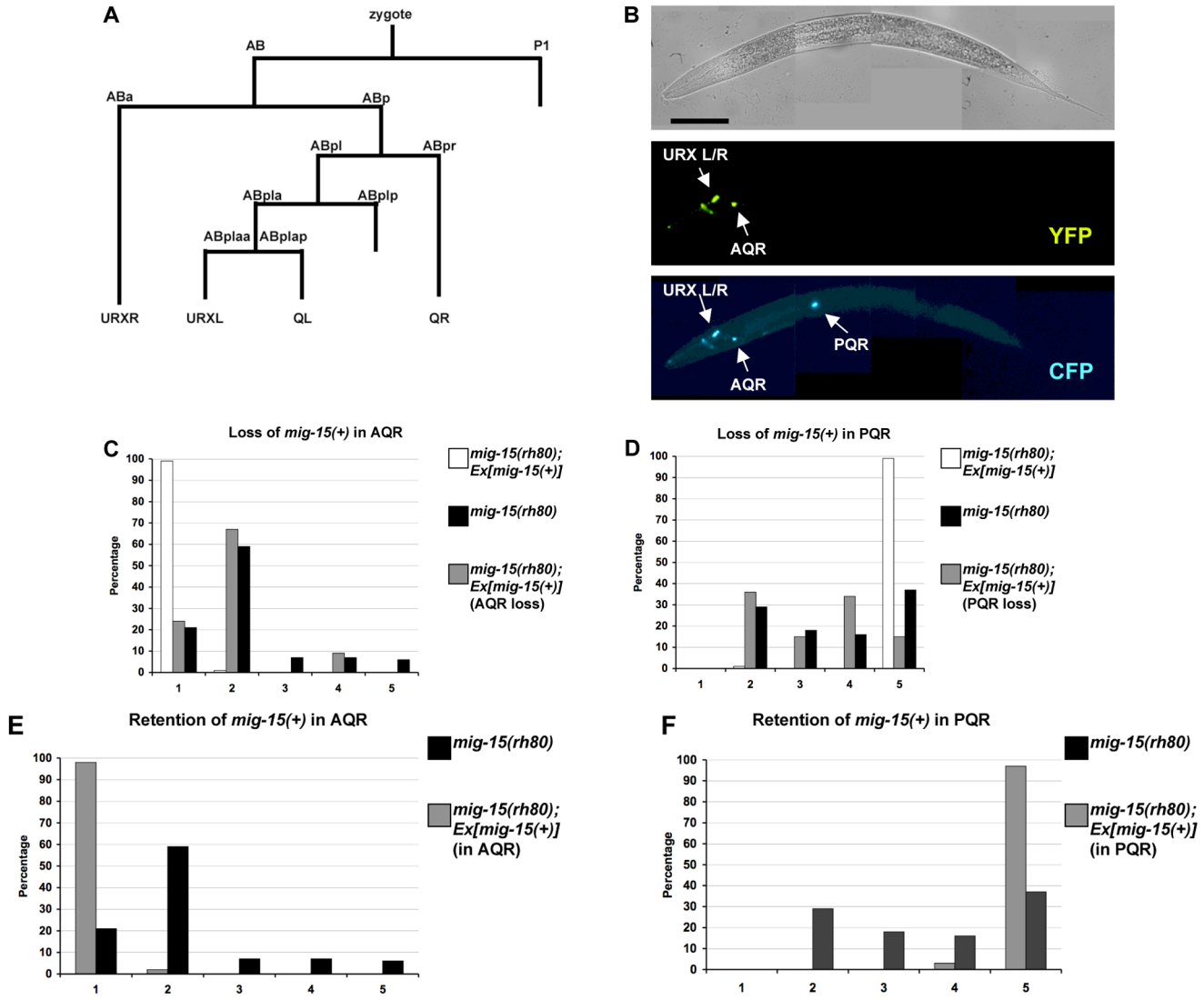

Figure 10. MIG-15 NIK kinase acts cell autonomously in AQR and PQR migration

(A) The cell lineage map for the *gcy-32*-expressing cells. Not all divisions or cells are shown. (B) A mosaic animal that had lost the *mig-15(+)* transgene in the PQR neuron. The top micrograph is a Nomarski image. The middle micrograph shows that this animal has lost the *mig-15(+)* transgene in the PQR neuron as indicated by the lack of YFP expression in PQR. The bottom micrograph shows the position of AQR and PQR using an integrated *gcy-32::cfp* reporter. PQR reversed direction of migration. The scale bar in the top micrograph represents 50μm for all 3 micrographs in (B). (C–F) Quantitation of the final migratory positions of PQR and AQR in *mig-15(rh80)* and in mosaics.

Table 1

mig-15 polarity maintenance defects (~3–3.5 hours after hatching).

QL **Genotype**	**Normal polarization**	**Anterior extensions**	**Anterior/posterior polarization**	**No strong polarization**
mig-15(rh80) (63)	70%	14%	5%	11%
mig-15(rh148) (45)	62%	16%	13%	9%
QR Genotype	Normal polarization	Posterior extensions	Anterior/posterior polarization	No strong polarization
mig-15(rh80) (55)	65%	11%	11%	13%
mig-15(rh148) (48)	85%	8	0	7%